JGH Open Open Access An open access journal of gastroenterology and hepatology

JGHF Journal of Gastroenterology and Hepatology Foundation

doi:10.1002/jgh3.12513

ORIGINAL ARTICLE

Role of magnifying endoscopy with narrow-band imaging in the diagnosis of noninvasive gastric neoplasia

Keisuke Tanaka,* Shinya Maekawa,* Takashi Yoshida,* Tatsuya Yamaguchi,* Shinichi Takano,* Shuya Matsuda,* Hiroshi Hayakawa,* Yasuaki Ishida,* Masaru Muraoka,* Satoshi Kawakami,* Yoshimitsu Fukasawa,* Toru Kuno,* Fumihiko Iwamoto,* Yuya Tsukui,* Shoji Kobayashi,* Yukiko Asakawa,* Hiroko Shindo,* Mitsuharu Fukasawa,* Yasuhiro Nakayama,* Taisuke Inoue,* Tomoyoshi Uetake,* Masahiko Ohtaka,* Tadashi Sato,* Kunio Mochizuki† and Nobuyuki Enomoto*

*First Department of Internal Medicine, Faculty of Medicine and †Department of Pathology, Faculty of Medicine, University of Yamanashi, Yamanashi, Japan

Key words
cancer-related gene mutations, gastric adenoma, gastric intramucosal carcinoma, gastric noninvasive neoplasia, magnifying narrow-band imaging.

Accepted for publication 12 February 2021.

Correspondence
Shinya Maekawa, First Department of Internal Medicine, Faculty of Medicine, University of Yamanashi, 1110, Shimokato, Chuo, Yamanashi 409-3898, Japan.
Email: maekawa@yamanashi.ac.jp

Declaration of conflict of interest: The authors declare no conflicts of interest associated with this manuscript.

Funding support: Japan Agency for Medical Research and Development

Abstract

Background and Aim: There are no globally approved, distinguishing criteria enabling the classification of gastric adenomas and intramucosal carcinomas for differential diagnosis of noninvasive neoplasia (NIN).

Methods: Next-generation sequencing of 50 cancer-related genes was undertaken on 68 pathologically diagnosed microdissected gastric neoplasms (25 adenomas, 27 intramucosal carcinomas, and 16 submucosal carcinomas) obtained during endoscopic submucosal dissection. Findings from magnifying endoscopy with narrow-band imaging (M-NBI) of 52 NINs (the 25 adenomas and 27 intramucosal carcinomas) were compared with these data.

Results: Among all 68 neoplasms, the most frequently mutated genes were *APC* (76% in adenoma, 11.1% in intramucosal carcinoma, and 0% in submucosal carcinoma; $P < 0.001$) and *TP53* in intramucosal and submucosal carcinomas (8% in adenoma, 48.1% in intramucosal carcinoma, and 75% in submucosal carcinoma; $P < 0.001$). Dividing the NIN neoplasms into five groups according to their mutational status (A1: *APC* mutation, A2: *APC* + α mutation, B: *APC* + *TP53* mutation, C: *TP53* mutation, D: no mutation in either *APC* or *TP53*) resulted in almost identical diagnoses by pathology and M-NBI for groups A1 (12/13, 92%), C (12/13, 92%), and D (16/17, 94%) but not for groups A2 (3/7, 43%) or B (0/2, 0%). This finding implies that NINs with the *APC* + α mutation have carcinoma-like endoscopic features despite most being judged as adenomas by pathology.

Conclusion: A diagnosis of NINs by pathology or M-NBI in the subset of gastric tumors classified by cancer-related mutations is not completely identical, suggesting the possible additional role of M-NBI in diagnosing NINs. Further studies are needed to confirm this.

Introduction

Recent high-throughput cancer-related genetic analysis, using next-generation sequencing (NGS), has revealed molecular abnormalities in gastric cancer, and significant advances in personalized and precision medicine are now expected as a result.[1–5] Although these previous studies were mainly aimed at assessing advanced cancers, there are also some recent reports on early gastric carcinomas (GC) and adenomas. The most commonly mutated genes are *TP53*[6,7] in early GC and *APC* in adenomas.[8] Because cancer-related gene mutations are reflected in cancer biology, they may provide important information on the biological characteristics of these neoplasms.

In Europe and the United States, histopathological evidence of infiltration of neoplasms into the submucosa or deeper has been considered to indicate "carcinoma," whereas noninvasive neoplasias (NINs)[9–16] confined to the mucosa have been conventionally described as "dysplasia." However, in Japan, NINs have been classified into two pathological categories, "adenomas" and "intramucosal carcinomas," based on the nuclear and structural atypicality of the neoplastic cells and tissues.[16] In order to unify these discrepant diagnostic criteria, the Vienna classification[17] was proposed and revised in 2000[18] to reflect agreement to include "high-grade dysplasia" (as designated in Europe and the United States) and "intramucosal carcinoma" (in Japan) in the same category. Such NINs do have the potential for infiltrating the submucosa and require treatment; currently, endoscopic resection including endoscopic submucosal dissection (ESD) is widely accepted as the local treatment of choice

because of its low invasiveness and high control rate. However, despite such international agreements on the diagnosis of gastric NINs by pathology,[19] the differential diagnosis of gastric adenomas and gastric intramucosal carcinomas remains challenging in clinical practice. This is because of the diverse morphological features of NIN lesions and the lack of standardized diagnostic criteria to distinguish between adenomas and gastric intramucosal carcinomas,[16,17,20,21] especially in borderline cases.

In such a setting, recent advances in magnifying endoscopy with narrow-band imaging (M-NBI) have made it possible to distinguish between cancerous and noncancerous neoplasms without a pathological diagnosis.[22,23] In addition, M-NBI might be useful for the differential diagnosis of gastric adenoma and gastric intramucosal carcinoma.[24,25] In Japan, a "magnifying endoscopy simple diagnostic algorithm for early gastric carcinoma" (MESDA-G) has been proposed using M-NBI information on the demarcation line (DL), microvascular pattern (MVP), and microsurface pattern (MSP) of the neoplasm surface. The usefulness of this algorithm is gradually being acknowledged clinically.[26] However, in the context of the increasingly routine assessment of cancer-related mutations, it was unclear whether M-NBI findings from previous studies would provide any additional information useful for the accurate diagnosis of gastric NINs. The present study therefore investigated the relationships between pathology and M-NBI findings classified by the distribution of cancer-related mutations.

Methods

Patients and samples. A total of 68 lesions was included in this retrospective study. Histopathology indicated 25 gastric adenomas and 43 early GC (differentiated adenocarcinoma). Here, we focused on the differences between adenoma and intramucosal well-differentiated adenocarcinoma because it is often difficult to distinguish these forms by pathology. We therefore excluded undifferentiated adenocarcinoma. Among these 68 early GC, 27 were intramucosal, and 16 were submucosal. The lesions were resected by ESD at Yamanashi University Hospital from February 2011 to February 2016, with 68 lesions being the total number available over this time period. The histopathological diagnosis was determined according to the Japanese classification of GC, 3rd English edition,[27] by two independent expert pathologists (KM and MO). Helicobacter pylori infection status was determined by the presence of immunoglobulin G antibody in serum, ^{13}C-urea breath test, or tissue culture of biopsied samples.

This study was approved by the Human Ethics Review Committee of Yamanashi University, Faculty of Medicine.

Collection of samples, extraction of DNA, and analysis of somatic alterations. Tumor areas and neighboring nontumor areas were taken from consecutive sections of pathology-diagnosed specimens using laser capture microdissection (LCM). DNA was extracted from the cut tissue and semi-exhaustively searched for tumor-related genetic abnormalities using NGS and digital polymerase chain reaction (dPCR). Detailed methods of LCM, extraction of DNA, NGS, and dPCR are shown in Supplemental Methods.

Endoscopic procedures and analyses. Target lesions were observed under normal light, or optionally with indigo carmine dye, and then under M-NBI. From the M-NBI images, endoscopic diagnosis of the target lesions was made by three experienced endoscopists using MESDA-G.[26] For the endoscopic diagnosis of target lesions under M-NBI, it was first determined whether there was a clear DL at the border between the lesion and the surrounding mucous membrane. Next, the MVP of the lesion was determined as (i) regular, (ii) irregular, or (iii) absent. Similarly, the MSP was determined as (i) regular, (ii) irregular, or (iii) absent. An example is shown in Figure 1. The judgment made by two or more of the three endoscopists was recorded as the final endoscopic diagnosis.

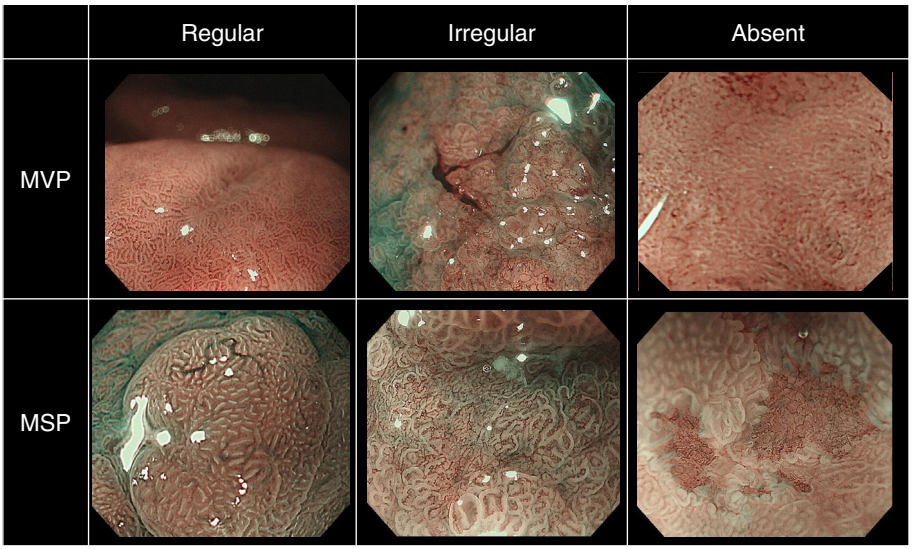

Figure 1 Gross morphology showing regular, irregular, and absence of a microvascular pattern (MVP) and microsurface pattern (MSP).

Table 1 Clinicopathologic characteristics of 25 adenomas and 43 early gastric cancer (EGC)

		EGC (n = 43)	
Age (years)†	Adenoma (n = 25)	Intramucosal GC (n = 27)	Submucosal GC (n = 16)
Gender, n (%)	72 (62–84)	73.5 (54–88)	73 (58–87)
Male	21 (84)	19 (70.4)	13 (81.3)
Female	4 (16)	8 (29.6)	3 (18.8)
Location, n (%)			
U	3 (12)	3 (11.1)	6 (37.5)
M	12 (48)	9 (33.3)	7 (43.8)
L	10 (40)	13 (48.1)	1 (6.3)
Remnant stomach	0	2 (7.4)	2 (12.5)
Size (mm)†	15 (6–60)	12 (6–29)	21 (6–42)
Macroscopic types, n (%)			
Elevated (I/IIa/IIa + IIc)	23 (92)	14 (54.6)	2 (12.5)
Depressed (IIc/IIc + IIa)	2 (8)	13 (48.1)	14 (87.5)
Color, n (%)			
Whitish or normal color	20 (80)	18 (66.7)	3 (18.8)
Reddish color	5 (20)	9 (33.3)	13 (91.2)
Histological classification, n (%)			
tub1 or tub1 > tub2		26 (96.3)	13 (81.2)
tub2 or tub2 > tub1		1 (3.7)	3 (18.8)

†Median (range).
GC, gastric cancer; L, lower third; M, middle third; U, upper third.

Statistical analysis. We compared baseline characteristics of the groups using Fisher's exact test for categorical variables. We used the Cochran–Armitage test to detect the trend between gastric mucin phenotypes and cancer-related mutations in early GC. P values of <0.05 by the two-tailed test were considered to indicate statistical significance.

Results

Clinicopathological characteristics of the gastric neoplasms. A total of 68 lesions from 68 patients was included in this retrospective study (Table 1): Histopathology defined 25 as gastric adenomas and 43 as early GC (differentiated adenocarcinomas). Of the latter, there were 27 intramucosal carcinomas and 16 submucosal carcinomas. Patients were mainly men in their 70s. Locations, macroscopic types, and color varied according to each neoplasm. There were 52 NINs (25 adenoma and 27 intramucosal GC).

Somatic mutations of cancer-related genes. Cancer-related mutations and their correlations with the clinicopathological background are shown in Figure 2. A list of mutations, mutation frequency, mutational effect, nucleotide change, amino acid change, and coverage identified in each adenoma lesion is shown in Table S1. Similarly, information on intramucosal carcinoma and submucosal carcinoma is detailed in Tables S2 and S3.

Cancer-related somatic gene mutations in histopathologically diagnosed gastric adenoma. A total of 34 mutations was found in 20 of 25 (80%) adenomas, with no mutations in the remaining 5 (20%) (Fig. 2). The most common and frequent mutation among the adenomas was in the *APC* gene as found in 19 cases (76.0%), in which mutations of genes other than *APC* were also detected in 7, including 2 *TP53*, 3 *KRAS*, 1 *FBXW7*, 1 *ATM* mutation, and 1 *CDKN2A* mutation. Of the 19 adenomas with *APC* mutations, 3 had >1 mutation in the *APC* gene. A single adenoma case had only an *SMO* mutation. These mutation patterns are shown in Figure 3 comprising 34 mutations, of which 11 were nonsense, 12 missense, and 11 frameshifts, with the latter observed only in the *APC* gene. Of the 23 point mutations found, 13 were C > T transitions, 7 were C > A transversions, 2 were C > G transversions, and 1 was an A > C transversion (Fig. 3).

Cancer-related somatic gene mutations in histopathologically diagnosed early gastric carcinoma. A total of 49 mutations was found in 34 (79.1%) of the 43 early GC, with no mutations found in the remaining 9 (20.9%). Of these 34 cases, 25 had a single mutation, and 9 had multiple mutations (Fig. 2). The most frequent mutation among early GC was in the *TP53* gene, found in 25 cases (58.1%). Stratifying early GC into intramucosal or submucosal carcinoma allowed comparison of the presence or absence of *TP53* mutations and multiple other mutations. However, there were no significant differences between the two groups regarding the presence or absence of the *TP53* mutation (P = 0.12). On the other hand, although there were also no significant differences between intramucosal and submucosal carcinomas with respect to the presence or absence of multiple mutations, there was a tendency for submucosal carcinoma to have multiple mutations (P = 0.057).

Of these 49 mutations (Fig. 2), 8 were nonsense, 35 missense, 2 frameshift and 2 nonframeshift indel, and 1 each of Splicesite and Stoploss, with the highest number of missense mutations. Of the 43 point mutations (Fig. 3), 29 were C > T

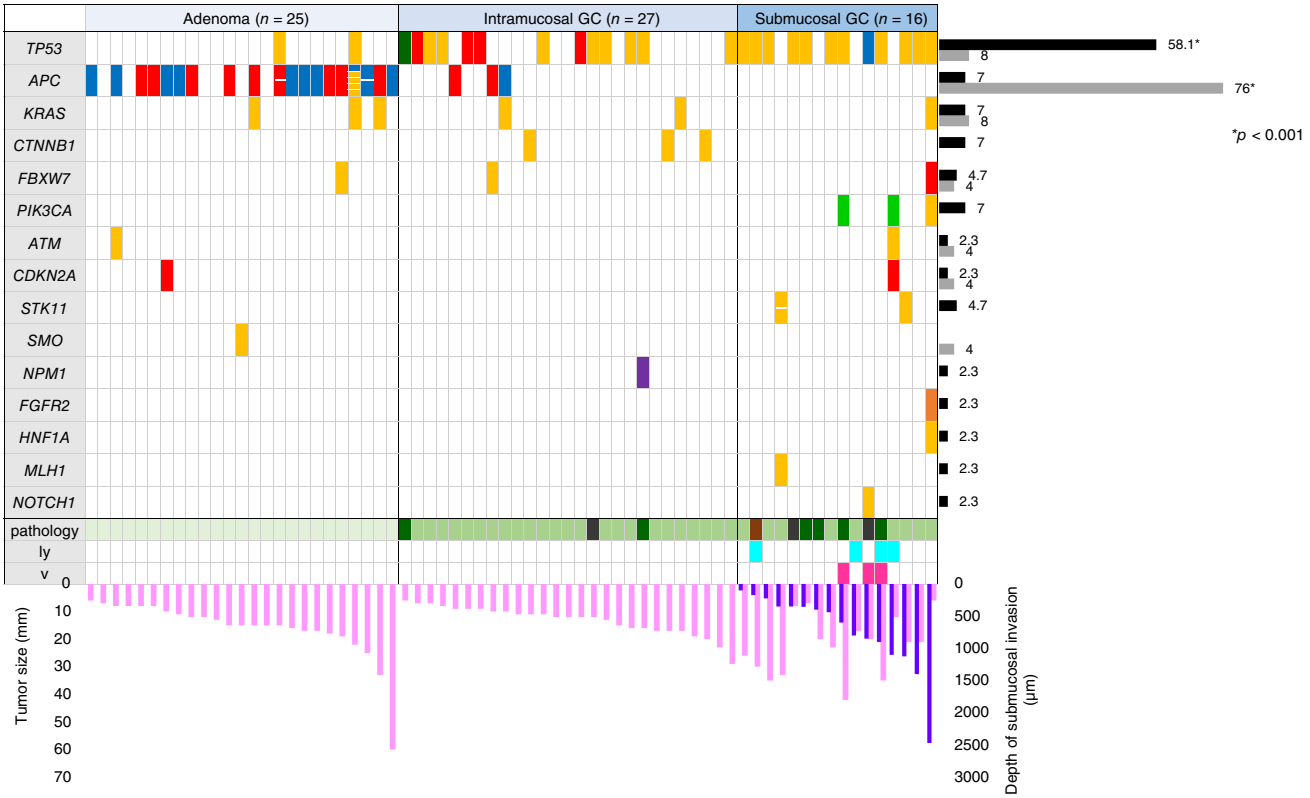

Figure 2 Distribution of somatic cancer-related gene mutations and clinicopathological findings in 68 gastric lesions (25 adenoma, 27 intramucosal gastric carcinoma (GC), and 16 submucosal GC). Mutation rates on the right axis are for the genes of 25 adenomas and 43 early gastric carcinomas (intramucosal gastric carcinoma + submucosal gastric carcinoma) (EGC). The depth of the pink bar represents neoplasm size, and the depth of the blue bar indicates the depth of submucosal invasion. Adenoma and intramucosal GC are sorted by neoplasm size. Submucosal GC are sorted by neoplasm depth. (■), EGC; (■), adenoma; (■), nonsense; (■), missense; (■), frame shift; (■), splice site; (■), stop loss; (■), non-frame indel; (■), adenoma; (■), tub1; (■), tub1 > tub2; (■), tub2 > tub1; (■), tub2. ly, lymphatic invasion; v, vascular invasion.

transitions, 4 were C > A transversions, 3 were C > G transversions, 2 were A > G transitions, 4 were A > T transversions, and 1 was an A > C transversion. Thus, as in the adenomas, C > T transition was the most common.

Comparison of mutations in histopathologically diagnosed adenoma and intramucosal carcinoma. The most commonly mutated genes in adenoma and intramucosal carcinoma were *APC* (76%, 19/25) and *TP53* (48.1%, 13/27), respectively, a significant difference ($P < 0.001$ and $P = 0.0019$). Seven adenomas and three intramucosal carcinomas had mutations in multiple genes, but there were no significant differences between the two ($P = 0.16$). In addition, the same combinations of mutations were found across adenomas and intramucosal carcinoma: *APC* + *KRAS* mutations in two adenomas and one intramucosal carcinoma and *APC* + *FBW7* mutations in one adenoma and one intramucosal carcinoma.

Magnifying endoscopy findings with narrow-band imaging, and conventional white-light imaging of 52 NIN neoplasms. All 52 neoplasms categorized as NINs had a DL. The presence or absence of irregular microvascular pattern (IMVP) and irregular microsurface pattern (IMSP) in 25 cases (a1–25) of adenoma and 27 cases (m1–m27) of intramucosal carcinoma was judged by three investigators, as shown in Table S4. Figure 4 summarizes the mutations, the profiles of IMVP and IMSP, and depression and redness evaluated by conventional white-light imaging of these 52 neoplasms. Overall, there were 30 IMVPs and 22 IMSPs, and all neoplasms with IMSP also had IMVP.

IMVP and/or IMSP were found in 6 of 25 (24%) adenomas and 24 of 27 (89%) intramucosal carcinomas ($P < 0.001$). The detection sensitivity of pathologically diagnosed intramucosal carcinomas by IMVP and/or IMSP was 89%, and the specificity was 76%.

In addition, a significant difference was recognized with respect to the presence of depression between the adenomas (2/25, 8%) and the intramucosal carcinomas (13/27, 48%) ($P = 0.0019$). On the other hand, there were no significant differences between the two groups regarding redness (20% in adenoma and 33.3% in intramucosal carcinoma, $P = 0.36$) (Fig. 4).

Relationships between mutations, endoscopic findings, and pathology in NIN. Of the 52 NINs, 11 had single *TP53* mutations, of which 10 were IMVP- and/or IMSP-positive (91%) with a pathological diagnosis of intramucosal carcinoma. Thirteen possessed a single *APC* mutation, with none

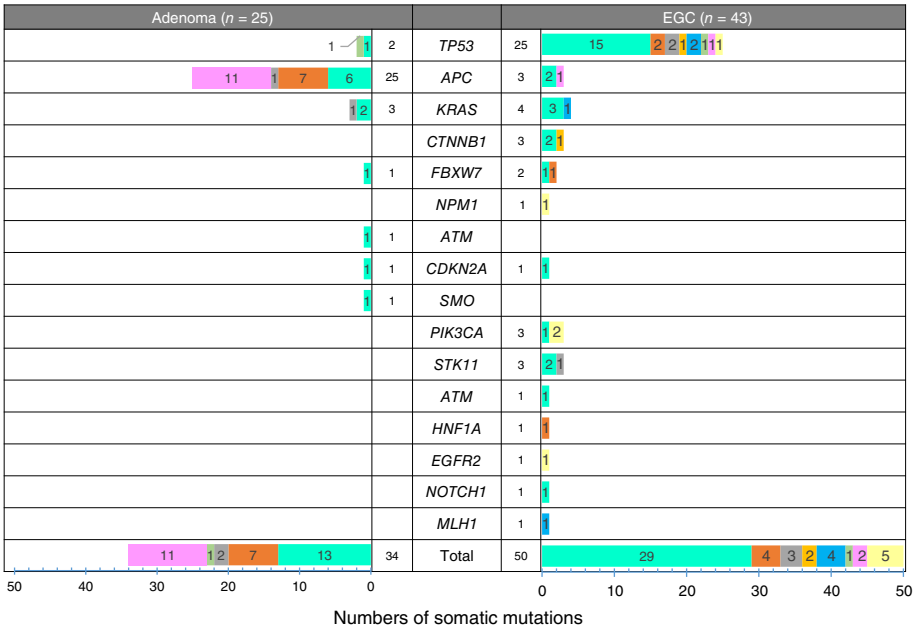

Figure 3 Numbers of mutations and mutational patterns of 68 gastric lesions (25 adenoma, 43 early gastric carcinoma [EGC]). (■), C > T (G > A); (■), C > A (G > T); (■), C > G (G > C); (■), A > G (T > C); (■), A > T (T > A); (■), A > C (T > G); (■), frame shift; (■), other non-syn.

displaying IMVP or IMSP. The pathological diagnoses of these 13 neoplasms were 12 adenomas and 1 intramucosal carcinoma. Moreover, in addition to the *APC* mutations, there were seven pathologically diagnosed adenomas carrying another mutation, within which IMVP and/or IMSP was recognized in six (86%) (Fig. 4). IMVP and/or IMSP findings were significantly more frequent in adenomas with *APC* + additional mutations (86%) than adenomas with a single *APC* mutation (0%) ($P < 0.001$) (Fig. 4).

In order to further investigate the relationship between mutations, pathological diagnosis, and M-NBI findings among NINs, we divided them into four groups according to their mutational patterns of *APC* and *TP53*, as follows: group A (*APC* mutation+/*TP53* mutation-, $n = 20$), group B (*APC* mutation+/*TP53* mutation+, $n = 2$), group C (*APC* mutation-/*P53* mutation+, $n = 13$), and group D (*APC* mutation-/*TP53* mutation-, $n = 17$). Group A was further subdivided into A1

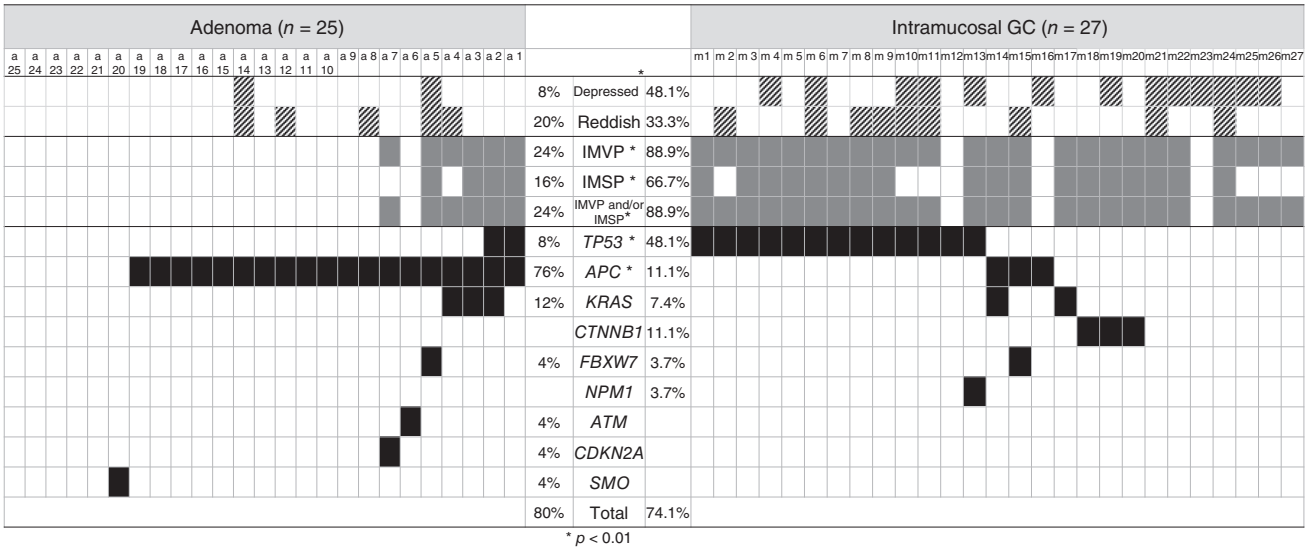

Figure 4 Magnifying narrow-band imaging and conventional white-light endoscopic findings and mutations in 25 adenomas and 27 intramucosal gastric carcinomas (GC). "Total" indicates the percentage of mutations observed in adenomas and intramucosal carcinomas. The *P* value was calculated using Fisher's exact test. (■), Conventional white light imaging; (■), magnifying narrow-band imaging; (■), somatic mutations. Depressed, macroscopic type 0-IIc or 0-IIc+IIa; IMSP, irregular microsurface pattern; IMVP, irregular microvascular pattern; Reddish, surface configuration red color change.

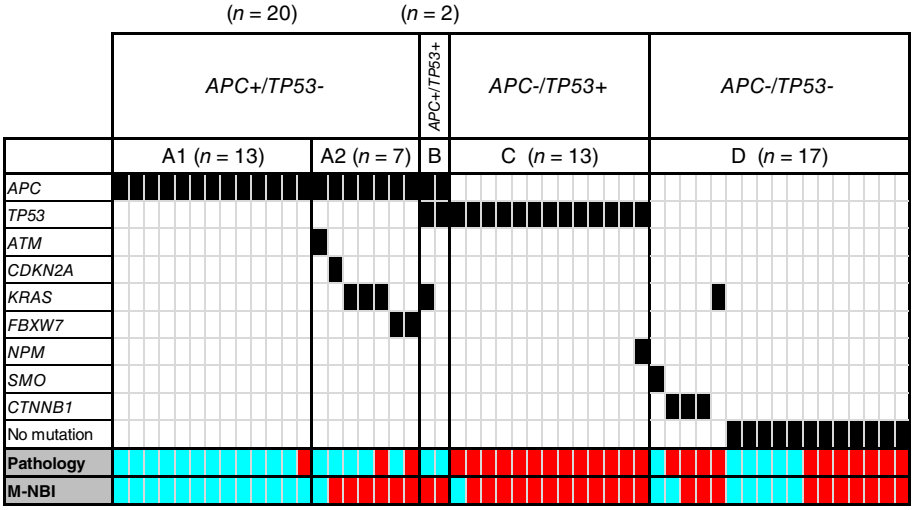

Figure 5 Relationship between pathology-based diagnosis and magnifying endoscopy with narrow-band imaging (M-NBI)-based diagnosis stratified by mutations in gastric noninvasive neoplasia. In the pathology and M-NBI lines, each red square was judged as cancer according to pathology criteria or the criteria of M-NBI, respectively. (■), Findings compatible with cancer; (■), findings incompatible with cancer.

(n = 13) and A2 (n = 7) according to the presence of other mutations. As shown in Figure 5, diagnoses of group A1 neoplasms were almost identical whether based on pathology or M-NBI (12/13, 92%), and all were judged to be adenomas. Similarly, diagnoses of group C neoplasms were almost identical by pathology and M-NBI (13/13, 100%), all judged to be intramucosal carcinoma. In group D, there was a mixture of neoplasms judged as adenoma and intramucosal carcinoma, and again, the diagnoses were almost identical whether by pathology or M-NBI (16/17, 94%). In contrast, the diagnosis by pathology was significantly different from M-NBI in group A2/B (3/9, 33%); in this case, most of these neoplasms were diagnosed as adenoma by pathology (7/9, 78%) but as carcinoma by M-NBI (8/9, 78%) (Fig. 5). Figure S1 shows M-NBI findings and images of several NINs in groups A1, A2, B, and C in comparison with pathological findings after classification according to cancer-related mutations.

Discussion

Because of the difficulty in differentially diagnosing gastric adenomas and intramucosal adenocarcinomas using the current diagnostic system based on pathology, here, we performed a semicomprehensive analysis of 50 cancer-associated genes in gastric NINs, with the main aim of determining whether additionally assessing M-NBI would assist in making a diagnosis. What is unique in this study is that it showed the relationship between pathology and M-NBI finding after classifying NINs through data on cancer-related mutations.

First, by analyzing adenoma, intramucosal carcinoma, and submucosal carcinoma diagnosed by pathology, we showed that mutations of the *APC* gene are characteristic of adenoma, while *TP53* mutations are characteristic of carcinoma. Importantly, because no *APC* mutation was observed in "infiltrative" submucosal carcinoma, *TP53* mutations are considered essential in gastric carcinogenesis, while adenoma-derived carcinoma, originating due to mutation of *APC*, is less likely to develop. In comparison with intramucosal gastric carcinoma, submucosal carcinoma has clearer pathological features of submucosal invasion and is easier to diagnose by pathology. Therefore, the contribution of *TP53* is evident, whereas the contribution of *APC* is weaker or even the opposite in the formation of submucosal carcinoma. This inverse relationship between *APC* and *TP53* and adenoma and carcinoma has been reported previously,[28] with a recent study reporting the stepwise correlation of *APC* and *TP53* along three steps of low-grade dysplasia, high-grade dysplasia, and early GC, as in our study.[29] Compared to these earlier studies, ours is more comprehensive in the context of a clear demonstration of *TP53* and *APC* mutations in early gastric carcinogenesis through the analysis of a larger number of samples exploiting advanced sample acquisition technologies and harvesting very small amounts of tissue using laser microdissection.

Next, we aimed to discover any additional roles of M-NBI data as a supportive tool in the diagnosis of NINs through cancer-related gene analysis. In a previous study reporting the differential diagnosis of gastric adenoma and adenocarcinoma on the basis of M-NBI, the sensitivity was 86–95% and the specificity was 38.9–88% when the diagnostic gold standard was set as pathological carcinoma.[24,25] In the present study, when pathology was similarly set as the diagnostic gold standard of NINs, the sensitivity was 89% and specificity was 76% for the diagnosis of carcinoma in 52 NINs using M-NBI (data not shown); this is similar to the previous report. On the other hand, classifying NINs by their cancer-related mutations resulted in assigning five categories according to the presence of *APC* and *TP53* mutations (Fig. 5). In this classification, the diagnosis of adenoma is most plausible for group A1-NINs with *APC+/TP53-* because most of these NINs were diagnosed as adenomas by both pathology and M-NBI. Similarly, carcinoma is most plausible for group C-NINs with *APC −/TP53+* because most of the NINs were diagnosed as carcinomas by both pathology and M-NBI. In contrast, the situation was different for *APC−/TP53-* NINs (group D). However, because the

cancer gene panel used in this analysis contained only 50 genes but not any previously reported driver genes such as *RHOA*, *ARID1A*, and *MUC6*,[1,24] precisely which genes are involved is unclear. Interestingly, however, the diagnosis by both modalities was almost identical for each NIN.

Compared to the essentially identical agreement between pathology and M-NBI diagnosis in groups A1 (92%, 12/13), C (92%, 12/13), and D (94%, 16/17), the diagnosis of carcinoma was more frequent by M-NBI than pathology in groups A2 (43%, 3/7) and B (0%, 0/2). Examining the difference between A2 and B more closely, four NINs diagnosed as adenoma by pathology in A2 were diagnosed as carcinoma by M-NBI, and two adenomas diagnosed by pathology in B were diagnosed as carcinoma by M-NBI. Regarding cancer-related mutations, A2 had mutations of *KRAS*, *FBXW7*, *ATM*, and *CDK2A* in addition to *APC*, and B had *TP53* mutations in addition to *APC*. In previous studies, the *FBXW7* mutation was associated with poor prognosis in advanced GC, *ATM* loss of function was associated with a 4–5-fold increase in the incidence of early GC by Genome-wide association studies (GWAS) analysis, and *CDKN2A* mutation was also associated with early GC,[30] while the role of *KRAS* mutation in gastric carcinoma is debatable.[28] Considering that the cancer-related mutations could be a reflection of tumor biology, it is possible that the NINs in groups A2 and B have a higher potential for malignancy compared to those with a single *APC* mutation (A1). This finding suggests an additional nonredundant role of M-NBI for the diagnosis of NINs.

Why did the pathological diagnosis and the M-NBI diagnosis differ in some cases? Both these diagnostic systems rely on the morphological features found in neoplasms, but they assess different observation items in that NIN diagnosis by pathology relies on the nuclear and structural atypia found in neoplasms, whereas the M-NBI relies on irregularities in microstructure and microvascularity on the surface. Currently, it is not clear whether this diagnostic discrepancy between pathology and M-NBI was caused by the differences in morphological changes observed in association with tumor progression or whether it was caused by differences in the ease of detectability of morphological changes between the two. In Figure S1 showing M-NBI images of several NINs, those in groups A2 and B seemed to have more malignant M-NBI features, especially in MVP findings, relative to A1. Further studies are needed to determine relationships among these morphological features found in pathology and M-NBI and cancer-related mutation status.

This study has some limitations. First, the number of cases is not large. Second, this is a cross-sectional study, and the longitudinal outcome of the patients with these NINs is unknown. Specifically, although it is suggested that NINs in groups A2 and B possessed a higher malignant potential than A1 NINs, it is uncertain whether these did progress to infiltrative submucosal carcinoma. In fact, the actual submucosal carcinomas in this study always had *TP53* mutations, whereas group A2-NINs did not. Further studies are needed to clarify these issues.

In conclusion, through comparisons of pathology and M-NBI for NINs in the context of cancer-related gene mutation data, we have documented that a single *APC* mutation was specific for gastric adenomas, while the *TP53* mutation was specific for gastric intramucosal carcinomas. Second, we showed that some NINs were diagnosed as adenomas by pathology but as intramucosal carcinomas by M-NBI, and such NINs with discrepant diagnoses had a characteristic profile of *APC* plus other mutation(s), different from the profiles found in the NINs without discrepant diagnoses. Although the clinical significance of these findings requires clarification in longitudinal studies, M-NBI findings are suggested to have an additional valuable role in the diagnosis of NINs.

References

1 Cancer Genome Atlas Research N. Comprehensive molecular characterization of gastric adenocarcinoma. *Nature*. 2014; **513**: 202–9.
2 Cui J, Yin Y, Ma Q *et al*. Comprehensive characterization of the genomic alterations in human gastric cancer. *Int. J. Cancer*. 2015; **137**: 86–95.
3 Hu N, Kadota M, Liu H *et al*. Genomic landscape of somatic alterations in esophageal squamous cell carcinoma and gastric cancer. *Cancer Res.* 2016; **76**: 1714–23.
4 Ichikawa H, Nagahashi M, Shimada Y *et al*. Actionable gene-based classification toward precision medicine in gastric cancer. *Genome Med.* 2017; **9**: 93.
5 Wang K, Yuen ST, Xu J *et al*. Whole-genome sequencing and comprehensive molecular profiling identify new driver mutations in gastric cancer. *Nat. Genet.* 2014; **46**: 573–82.
6 Fassan M, Simbolo M, Bria E *et al*. High-throughput mutation profiling identifies novel molecular dysregulation in high-grade intraepithelial neoplasia and early gastric cancers. *Gastric Cancer*. 2014; **17**: 442–9.
7 Yoshida T, Yamaguchi T, Maekawa S *et al*. Identification of early genetic changes in well-differentiated intramucosal gastric carcinoma by target deep sequencing. *Gastric Cancer*. 2019; **22**: 742–50.
8 Lim CH, Cho YK, Kim SW *et al*. The chronological sequence of somatic mutations in early gastric carcinogenesis inferred from multiregion sequencing of gastric adenomas. *Oncotarget*. 2016; **7**: 39758–67.
9 Rugge M, Bersani G, Bertorelle R *et al*. Microsatellite instability and gastric non-invasive neoplasia in a high risk population in Cesena, Italy. *J. Clin. Pathol.* 2005; **58**: 805–10.
10 Rugge M, Nitti D, Farinati F, di Mario F, Genta RM. Non-invasive neoplasia of the stomach. *Eur. J. Gastroenterol. Hepatol.* 2005; **17**: 1191–6.
11 Testino G. Gastric precancerous changes: carcinogenesis, clinical behaviour immunophenotype study and surveillance. *Panminerva Med.* 2006; **48**: 109–18.
12 Cassaro M, Rugge M, Tieppo C *et al*. Indefinite for non-invasive neoplasia lesions in gastric intestinal metaplasia: the immunophenotype. *J. Clin. Pathol.* 2007; **60**: 615–21.
13 Kato M, Nishida T, Tsutsui S *et al*. Endoscopic submucosal dissection as a treatment for gastric noninvasive neoplasia: a multicenter study by Osaka University ESD Study Group. *J. Gastroenterol.* 2011; **46**: 325–31.
14 Nishida T, Tsutsui S, Kato M *et al*. Treatment strategy for gastric non-invasive intraepithelial neoplasia diagnosed by endoscopic biopsy. *World J. Gastrointest. Pathophysiol.* 2011; **2**: 93–9.
15 Ojima T, Takifuji K, Nakamura M *et al*. Complications of endoscopic submucosal dissection for gastric noninvasive neoplasia: an analysis of 647 lesions. *Surg. Laparosc. Endosc. Percutan. Tech.* 2014; **24**: 370–4.
16 Kato M. Diagnosis and therapies for gastric non-invasive neoplasia. *World J. Gastroenterol.* 2015; **21**: 12513–8.
17 Schlemper RJ, Riddell RH, Kato Y *et al*. The Vienna classification of gastrointestinal epithelial neoplasia. *Gut*. 2000; **47**: 251–5.
18 Stolte M. The new Vienna classification of epithelial neoplasia of the gastrointestinal tract: advantages and disadvantages. *Virchows Arch.* 2003; **442**: 99–106.

19 Schlemper RJ, Kato Y, Stolte M. Diagnostic criteria for gastrointestinal carcinomas in Japan and Western countries: proposal for a new classification system of gastrointestinal epithelial neoplasia. *J. Gastroenterol. Hepatol.* 2000; **15**: G49–57.
20 Sung JK. Diagnosis and management of gastric dysplasia. *Korean J. Intern. Med.* 2016; **31**: 201–9.
21 Kitaichi T, Dohi O, Fujita Y *et al*. Clinical and pathological challenges in the diagnosis of gastric-type differentiated adenocarcinoma in the stomach: a study of endoscopic submucosal dissection cases. *Digestion*. 2019; **99**: 301–9.
22 Yao K, Anagnostopoulos GK, Ragunath K. Magnifying endoscopy for diagnosing and delineating early gastric cancer. *Endoscopy*. 2009; **41**: 462–7.
23 Yao K, Doyama H, Gotoda T *et al*. Diagnostic performance and limitations of magnifying narrow-band imaging in screening endoscopy of early gastric cancer: a prospective multicenter feasibility study. *Gastric Cancer*. 2014; **17**: 669–79.
24 Maki S, Yao K, Nagahama T *et al*. Magnifying endoscopy with narrow-band imaging is useful in the differential diagnosis between low-grade adenoma and early cancer of superficial elevated gastric lesions. *Gastric Cancer*. 2013; **16**: 140–6.
25 Nonaka T, Inamori M, Honda Y *et al*. Can magnifying endoscopy with narrow-band imaging discriminate between carcinomas and low grade adenomas in gastric superficial elevated lesions? *Endosc. Int. Open*. 2016; **4**: E1203–E10.
26 Muto M, Yao K, Kaise M *et al*. Magnifying endoscopy simple diagnostic algorithm for early gastric cancer (MESDA-G). *Dig. Endosc.* 2016; **28**: 379–93.
27 Sano T, Aiko T. New Japanese classifications and treatment guidelines for gastric cancer: revision concepts and major revised points. *Gastric Cancer*. 2011; **14**: 97–100.
28 Lee JH, Abraham SC, Kim HS *et al*. Inverse relationship between APC gene mutation in gastric adenomas and development of adenocarcinoma. *Am. J. Pathol.* 2002; **161**: 611–8.
29 Rokutan H, Abe H, Nakamura H *et al*. Initial and crucial genetic events in intestinal-type gastric intramucosal neoplasia. *J. Pathol.* 2019; **247**: 494–504.
30 Yokobori T, Mimori K, Iwatsuki M *et al*. p53-Altered FBXW7 expression determines poor prognosis in gastric cancer cases. *Cancer Res.* 2009; **69**: 3788–94.

Supporting information

Additional supporting information may be found in the online version of this article at the publisher's website:

Appendix S1. Supporting information.

Table S1. Genetic mutations identified in 25 gastric adenoma lesions.
Table S2. Genetic mutations identified in 27 intramucosal GC lesions.
Table S3. Genetic mutations identified in 16 submucosal GC lesions.
Table S4. Results of decision by three doctors, based on magnifying endoscopic findings.

Figure S1. Images of gastric noninvasive neoplasias (NINs) using magnifying endoscopy with narrow-band imaging (M-NBI) in comparison with pathological findings stratified according to cancer-related mutations. A1: *APC* mutation, A2: *APC* + α mutation, B: *APC* + *TP53* mutation, C: *TP53* mutation. Arrows indicate demarcation line. MSP, microsurface pattern; MVP, microvascular pattern.